



## Multilayered Hybrid Nanofibers as Extreme Ultraviolet Target Irradiated with Low Energy Nd:YAG Laser

LIQIN GE<sup>1,2,\*</sup> and JIANYU JI<sup>1</sup>

<sup>1</sup>State Key Laboratory of Bioelectronics, School of Biological Science and Medical Engineering, Southeast University, Nanjing 210096, P.R. China

<sup>2</sup>Institute of Laser Engineering, Osaka University, 2-6 Yamada-oka, Suita, Osaka 565-0871, Japan

\*Corresponding author: Tel/Fax: +86 25 83795635; E-mail: geliqin7455@yahoo.com.cn

(Received: 3 July 2010;

Accepted: 17 January 2011)

AJC-9488

The extreme ultraviolet (EUV) light source with a wavelength of 13.5 nm has been believed to be the next generation of light source, which can be produced by laser produced plasmas. By now, Xe, Li, or Sn contained compounds have been used as the target materials, among which Sn target has attracted great attentions for its relative high conversion efficiency, for relatively lower laser intensity of *ca.* 1010 W/cm<sup>2</sup>. In this paper, we reported a new type of Sn contained nanofibers as extreme ultraviolet target induced with low energy Nd:YAG laser. The nanofibers were fabricated through the combination of the layer-by-layer technique with the electrospinning method. SEM image shows that the obtained multilayer hollow fibers were collapsed because of the solvent evaporation which was consistent with previous results.

**Key Words:** Extreme ultraviolet, Layer-by-layer, Electrospinning, Nanofibers.

### INTRODUCTION

Extreme ultraviolet (EUV) emission from laser plasmas has been extensively studied in recent years, as a candidate for light sources for EUV lithography<sup>1</sup>. Development of a high-power and clean EUV light source is a critical issue. Nd:YAG lasers were used which have an excellent potential in producing high peak-power laser pulses that are suitable for heating plasmas, resulting in strong EUV emission with reasonably high repetition rates. The EUV lithography system requires, at the source point, more than 300 W power of 13.5 nm light within a 2 % bandwidth (BW) and  $1 \times 10^{11}$  shots of life time under 10 kHz operation. Laser-produced plasma is an attractive light source for the EUV lithography in terms of its brightness and compactness. Various materials, *e.g.*, Li, Xe and Sn, were investigated to obtain sufficient EUV conversion efficiency (CE) and also power. Laser-produced Sn plasmas<sup>2</sup>, especially low density Sn plasmas<sup>3-7</sup>, are an attractive 13.5 nm light source due to its compactness and high emissivity, it has a highly intense emission peak at 13.5 nm, thus much effort is devoted to the development of the Sn-based EUV light source. Until now, there is no practical EUV light source system are investigated that can satisfy with the requested specifications for the high-volume-production of semiconductors due to several technological difficulties.

Polymer nanofibers can be used in filters, sensors, bio-catalysts, protective clothing, wound dressings, artificial blood vessels, controlled drug delivery and tissue growth applications<sup>8-10</sup>.

A rich variety of methods have been introduced to obtain nanotubes from all kinds of materials. The layer-by-layer (LBL) technique based on electrostatic forces gifts a controllable approach for surface coating with a designable layer structure, defined wall thickness and size. With this method, a variety of polyions including synthetic and natural materials have been used to construct polyelectrolyte multilayer microcapsules, which provide hollow capsules with special functions, such as catalysts, reaction cages, controlled permeability and drug carriers<sup>11-17</sup>. Electrospinning is a straightforward, cost-effective method to produce novel fibers with diameters ranging from nanometer to micrometer. The obtained fibers have very high continuous surface areas compared with other materials, for example spheres, slices and nanotubes. It has regained a great deal of attention due to a surge of interest in nanotechnology as continuous ultrafine fibers or fibrous structures of various polymers can be fabricated with diameters in the range from several micrometers down to tens of nanometers<sup>18-20</sup>. Carsuo and co-workers ever reported to obtain hollow multilayer polyelectrolyte nanofibers by layer-by-layer then removed the coral template nanofiber in the solution<sup>20</sup>. In our group, we have reported the fabrication of the hollow multilayered polyelectrolyte nanofiber by layer-by-layer technique and its application<sup>21-24</sup>. The coral template polystyrene (PS) nanofibers were obtained by electrospun method. Generally, poly(styrenesulfonate, sodium salt) (PSS) and poly(allylamine hydrochloride) (PAH)

were selected as shell materials because they are easily to form thin films and then the template PS nanofibers were removed by the organic solvent. The fabrication procedure was illustrated in **Scheme-I**. Since nanofibrous mats consist of many fibers, the formation of only one fiber and its' cross-section diagram were illustrated in **Scheme-I** in order that one can easily understand the procedure. In previous report<sup>6</sup>, we have reported to employ SnO<sub>2</sub> nanofibers as EUV target. To continue this study, we will study the fabrication of tin dioxide nanoparticles contained hollow nanofibers and employ it as EUV target irradiated with low energy Nd:YAG laser.

## EXPERIMENTAL

Poly(styrenesulfonate) sodium salt, (PSS,  $M_w$  70,000), poly (allylamine hydrochloride) (PAH,  $M_w$  70,000) and polystyrene were bought from Aldrich. PSS and PAH are polyelectrolytes and their chemical structures are shown in previous report<sup>25</sup>. Tin dioxide powder (average size is 250 nm as a catalog value) was obtained from Hosokana micron (Hirakata, Japan). The water used in all experiments was prepared in a three-stage Millipore Milli-Q Plus 185 purification system and had a resistivity higher than 18.2 M $\Omega$  cm<sup>-1</sup>.

**Preparation of tin dioxide monodispersed solution:** The tin dioxide nanoparticles were dispersed into an aqueous solution with pH 8.3 and ultrasonicated for 0.5 h. Tin dioxide nanoparticles are negatively charged when they are dispersed into pH 8.3 solution because its isoelectric point is about 6.7. Then they were kept at room temperature overnight. SEM image of the SnO<sub>2</sub> nanoparticles and their size distributions were reported in previous report<sup>25</sup>.

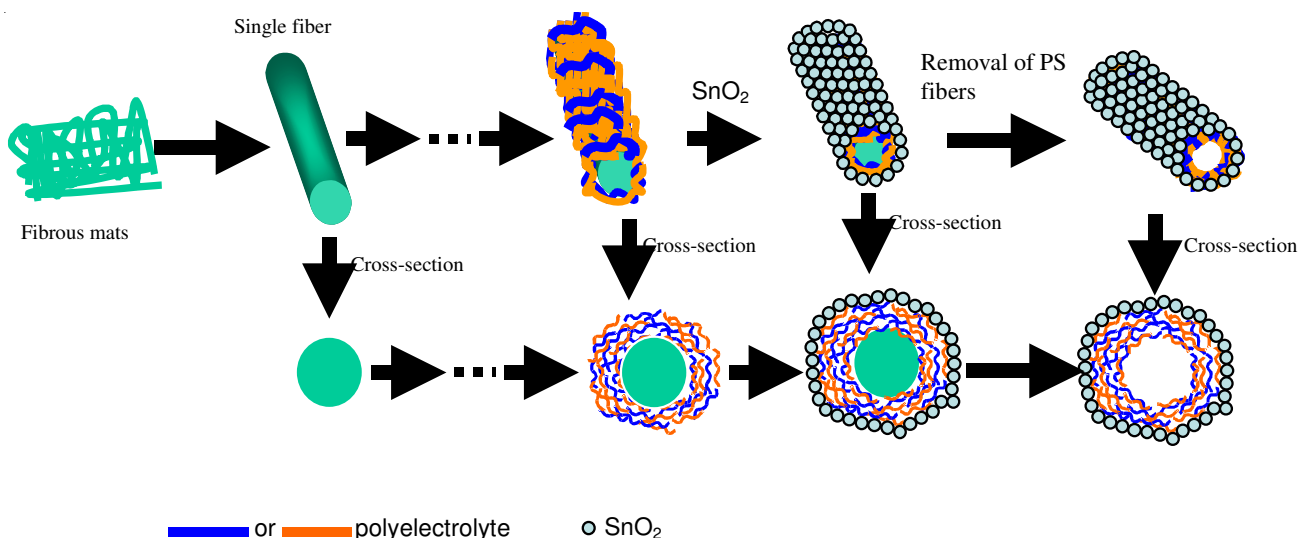
**Fabrication of polystyrene nanofibrous mats by electrospinning:** Polystyrene nanofibrous mats were prepared from a tetrahydrofuran/*N,N*-dimethyl formamide (DMF) mixed solution. As a typical procedure, 9.32 mL of THF/DMF solution containing 1.5 g of polystyrene ( $M_w = 185,000$  g/mol) was mixed for 2 h to get a viscous gel. It was quickly loaded into a syringe equipped with a five gauge stainless needle, which was connected to a high-voltage supply capable of generating voltage up to 35 kV. The feeding rate of the precursor

solution was controlled by using an automatic syringe pump. A plate used as the collector was placed 10 cm from the tip of the needle for the collection of the nanofibers. The solution on the tip of the needle was ejected as fibers under a strong electric field towards the collector. About the fibrous preparation method, details were shown in ref.<sup>26</sup>.

**Construction of hollow multilayer polyelectrolyte nanofibrous mats:** Poly(styrenesulfonate, sodium salt) and poly(allylamine hydrochloride) solution used for adsorption were prepared in Milli-Q water with a concentration 1 mg/mL in 0.5 M NaCl. An agglomerate of PS fibrous mat was selected as template and immersed into PAH solution and PSS solution alternatively. In every step, 0.5 h was left for adsorption and then rinsed by abundant water. The outermost layer is PAH, which is positively charged in order to bind the negatively charged tin dioxide nanoparticles in the next step. When five (PAH/PSS)<sub>2</sub>/PAH layers were finished and then the nanofibers were immersed into tin dioxide nanoparticle suspension for 1 h in order that the tin dioxide nanoparticles can be assembled on the fibers. Multilayer polymer/tin dioxide hybrid coated PS fibers were immersed into THF (2 mL) solution and left 50 min to remove the PS core. In order to remove the excess solution, the sample was centrifuged at 10,000 rpm for 3 min and then washed by THF for 2 times. Finally, the sedimentations were dispersed into water for next measurement.

**Scanning electronic microscope (SEM) observations:** Scanning electronic microscope images were obtained using a Jeol JSM-7400F field-emission scanning electron microscope operated at an accelerating voltage of 2 kV in the gentle-beam mode (ultralow accelerating voltage and high resolution). The PS sample was coated with platinum to improve the conductivity when observed by the SEM.

**Laser irradiation of the targets:** The EUV emission from the capsule was irradiate by Nd:YAG laser. As a photon detector, a liquid nitrogen cooled CCD (charge coupled device) camera was installed in the EUV spectrometer and an emission spectrum was obtained simultaneously. The laser energy is 176 mJ, the pulse is 2.88 ns and the laser intensity is  $3.10 \times 10^{10}$  W/cm<sup>2</sup>. The focal spot diameter is 500  $\mu$ m.



**Scheme-I:** Scheme for the fabrication of the multilayer hollow tin dioxide nanoparticles contained fibers

## RESULTS AND DISCUSSION

The typically electrospun nanofibrous mats which compose of polymer nanofibers possess a three-dimensional structure with pores in micro and sub-micro size. In this research, electrospinning technique was employed to obtain PS nanofibrous mats<sup>26</sup>, which were used as the template whose microscopic structure is shown in Fig. 1. It was observed that the electrospun fibers were weaved to form a porous membrane. The distribution of fiber's diameters was in the range from 1840-2600 nm and the average size is about 2200 nm. Generally, the surface-area-to-volume ratio of the porous mat is one to two orders of the magnitude higher than that of the flat thin films<sup>27</sup>. Fig. 1a is the SEM image of the fibers in a low magnification view and Fig. 1b shows the high magnification, one can find in Fig. 1b that the pure PS nanofiber has a smooth surface. According to previous results, negatively charged polymers and positively charged polymer can be alternatively assembled on the colloidal particles and PS fibers. In this experiment, the similar method was employed to form multilayer polyelectrolyte films on the fibers. Firstly, the mat was immersed into PAH solution and PSS solution at a concentration of 1 mg/mL, 0.5 M NaCl aqueous solutions, alternatively. In every step, 0.5 h was left for adsorption and then rinsed with abundant water. The first layer was selected as PAH layer because PS fibers were negatively charged<sup>12</sup>. The morphology (PAH/PSS)<sub>2</sub>/PAH coated PS fibers were shown in Fig. 2. From Fig. 2a, one can find after coated with five (PAH/PSS)<sub>2</sub>/PAH layers, the morphologies of the fibers were kept well which means that multilayer polyelectrolyte films were mainly formed only on the surface of the nanofibers. Fig. 2b shows that the fibrous surface becomes rougher after coating, which means that multilayered films were deposited on the fibrous surface successfully. FTIR spectra about the coating were reported in previous publication<sup>21</sup>. Fig. 3 shows the SEM image of hybrid polymer/SnO<sub>2</sub> coated PS nanofibers. Fig. 3a is the SEM image with low magnification and Fig. 3b is the SEM image with high magnification. From Fig. 3a, one can find after coated with six (PAH/PSS)<sub>2</sub>/PAH/SnO<sub>2</sub> layers, the morphologies of the fibers were still kept well which means that multilayer polyelectrolyte films and the nanoparticles were still mainly formed only on the surface of the nanofibers. Fig. 3b shows clearly that the tin dioxide nanoparticles were assembled on the PS fibers. In previous report<sup>25</sup>, SnO<sub>2</sub> nanoparticles can be assembled on the capsules which are consistent with this result. Fig. 4a and Fig. 4b shows the SEM images of the obtained hollow polyelectrolyte nanofibers with low and high magnification. They are collapsed during the sample preparation because of the solvent evaporation. According to previous reports<sup>13-16,21,25</sup>, hollow multilayered polyelectrolyte capsules obtained by layer-by-layer method will collapse after it is dried because of the inner solvent evaporation. It is consistent with present result. Fig. 5(a-b) shows the SEM image of the SnO<sub>2</sub> nanoparticles contained hollow multilayer hybrid nanofibers with a low and high magnification. Comparing Fig. 5b with Fig. 4b, one can easily find that SnO<sub>2</sub> nanoparticles were assembled on the fibrous surface. **Scheme-II** shows a schematic diagram of the experimental setup. A hybrid nanofibrous film target with a size about 3 mm × 3 mm

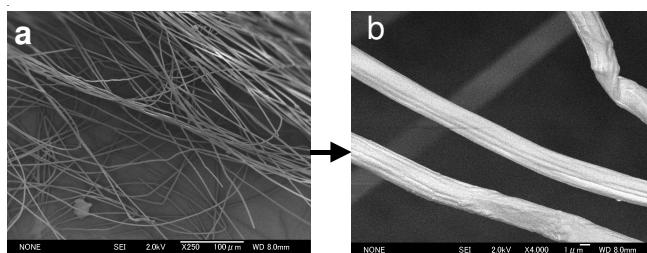


Fig. 1. SEM image of the PS fiber with a: (a) low magnification (b) high magnification

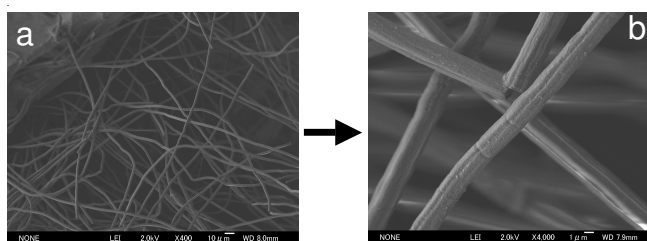


Fig. 2. SEM image of PS (PAH/PSS)<sub>2</sub>/PAH with a: (a) low magnification (b) high magnification

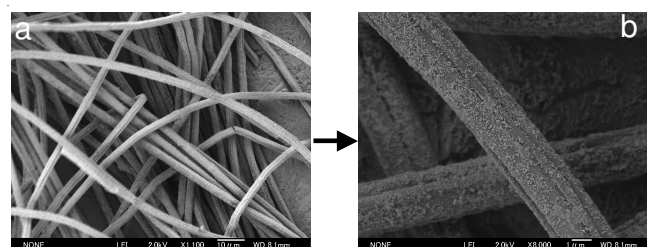


Fig. 3. SEM image of PS (PAH/PSS)<sub>2</sub>/PAH/SnO<sub>2</sub> with a: (a) low magnification (b) high magnification

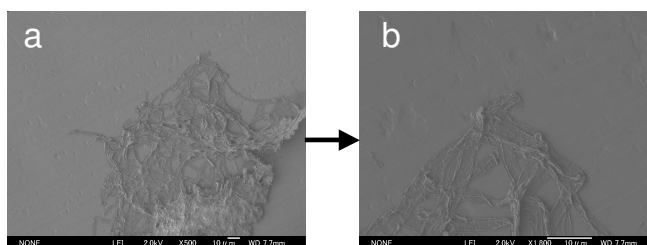


Fig. 4. SEM image of (PAH/PSS)<sub>2</sub>/PAH hollow nanofibers with a: (a) low magnification (b) high magnification

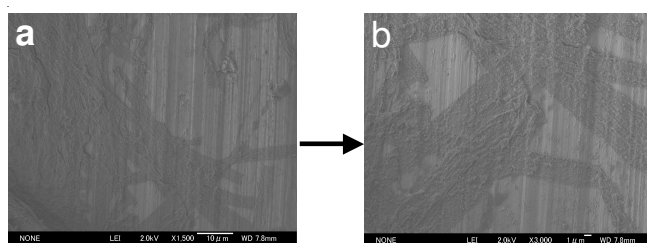
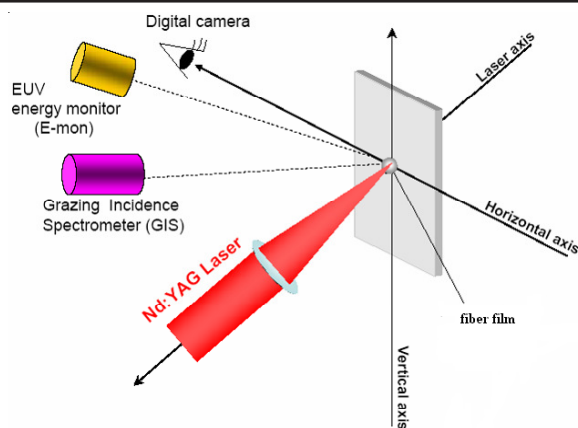


Fig. 5. SEM image of (PAH/PSS)<sub>2</sub>/PAH/SnO<sub>2</sub> hollow hybrid nanofibers with a: (a) low magnification (b) high magnification

was fixed on the glass slide in the vacuum chamber. During the operation of the jet, a pressure in the chamber was maintained less than 1 Pa. A set of silicon substrates was placed at 30 cm from the plasma area inside a chamber to monitor the debris. Absolute in-band EUV emission energy was measured by use of a EUV energy meter, which consisted of a photodiode, a Mo/Si mirror and a Zr filter. All of the components were





**Scheme-II:** Schematic diagram of the experimental setup with a: (a) low magnification (b) high magnification

calibrated. A flat-field grazing incidence spectrometer with an unequally ruled 1200 grooves/mm grating was positioned at  $45^\circ$  with respect to the incident laser axis. A micro-channel plate coupled with the spectrometer was used to detect the EUV spectra. Spectral resolution was 0.06 nm at 13.5 nm. The incident angle of laser beam was normal to the target front face<sup>1-6</sup>. Fig. 6 shows the EUV spectra emitted from the laser-produced plasmas, which is a typical one to provide highest conversion efficiency from laser to EUV light. A peak exists at 13.5 nm which is close to the previously reported wavelength<sup>5</sup>. Unfortunately we cannot conclude the conversion efficiency from laser to EUV light because angular distribution measurements are necessary to estimate it, although the spectrum has a considerable efficient intensity. Furthermore, the present EUV emission has 0.5 nm of half width which is narrowest the previous data for 10.6  $\mu\text{m}$  irradiation (1.5-2.0 nm for tin film<sup>3,4</sup> and 1 nm for a tin cavity<sup>5</sup>). The present nanofibrous sheets can produce EUV spectra induced with low density Nd:YAG laser. Such CE value means the obtained fibers may be employed as potential EUV target material in the future comparing with the previous results<sup>1-7</sup>.

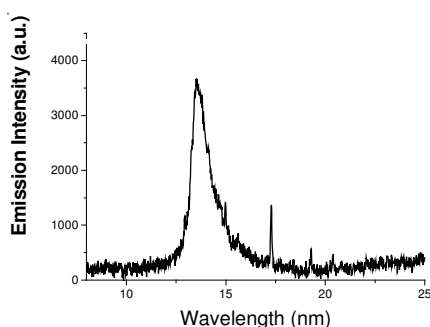


Fig. 6. EUV spectra emitted from the laser-produced plasmas

## Conclusion

Hollow multilayered hybrid polymer/inorganic nanofibers were fabricated through the combination of the layer-by-layer technique with the electrospinning method. The obtained hollow multilayered hybrid nanofibers can produce EUV spectra induced by Nd:YAG laser. SEM image shows that SnO<sub>2</sub> nanoparticles on the fibrous mats are continuous. This approach may also have application for the continuous providing target,

which is very important for the industrial application. In the future, we will try to control some important factors such as microstructure, density, anisotropy and mass, which have effects on the EUV transform efficiency, angular distribution and debris. And, also tried to improve the CE with high energy laser source.

## ACKNOWLEDGEMENTS

This work was performed under the Joint Research of Institute of Laser Engineering, Osaka University and was partly supported by the JSPS-CAS Core-University Program in the field of "Plasma and Nuclear Fusion". Liqin Ge thanks for the financial support from the Excellent Young Teacher Supporting Program for Teaching and Researching from Southeast University, Nanjing, P.R. China. One of the authors (Liqin Ge) also thanks for Profs. Nagai keiji, Hiroaki Mishimura, Yasukazu Izawa and Takayoshi Norimatsu's support to provide the experimental set up to finish the experiment.

## REFERENCES

1. A. Sasaki, K. Nishihara, M. Murakami, F. Koike, T. Kagawa, T. Nishikawa, K. Fujima, T. Kawamura and H. Furukawa, *Appl. Phys. Lett.*, **85**, 5857 (2004).
2. H. Tanaka, A. Matsumoto, K. Akinaga, A. Takahashi and T. Okada, *Appl. Phys. Lett.*, **87**, 041503 (2005).
3. Q.C. Gu, K. Nagai, T. Norimatsu, S. Fujioka, H. Nishimura, K. Nishihara, N. Miyanaga and Y. Izawa, *Chem. Mater.*, **17**, 1115 (2005).
4. T. Okuno, S. Fujioka, H. Nishimura, Y. Tao, K. Nagai, Q. Gu, N. Ueda, T. Ando, K. Nishihara, T. Norimatsu, N. Miyanaga, Y. Izawa, K. Mima, A. Sunahara, H. Furukawa and A. Sasaki, *Appl. Phys. Lett.*, **88**, 161501 (2006).
5. K. Nagai, Q.C. Gu, Z.Z. Gu, T. Okuno, S. Fujioka, H. Nishimura, Y.Z. Tao, Y. Yasuda, M. Nakai and T. Norimatsu, *Appl. Phys. Lett.*, **88**, 094102 (2006).
6. C. Pan, Z.Z. Gu, K. Nagai, T. Norimatsu, T. Birou, K. Hashimoto and Y.J. Shimada, *J. Appl. Phys.*, **100**, 016104 (2006).
7. K. Nagai, D. Wada, M. Nakai and T. Norimatsu, *Fusi Sci. Technol.*, **49**, 686 (2006).
8. A.P. Alivisatos, *Science*, **271**, 933 (1996).
9. S. Iijima, *Nature*, **354**, 56 (1991).
10. Y. Zhou, M. Freitag, J. Hone, C. Staii and A.T. Johnson, *Appl. Phys. Lett.*, **83**, 3800 (2003).
11. E. Donath, G.B. Sukhorukov, F. Caruso, S.A. Davis and H. MÖhwald, *Angew. Chem.*, **37**, 2201 (1998).
12. G.B. Sukhorukov, L. Dane, J. Hartmann, E. Donath and H. MÖhwald, *Adv. Mater.*, **12**, 112 (2000).
13. L.Q. Ge, H. MÖhwald and J.B. Li, *Chem. Eur. J.*, **9**, 2589 (2003).
14. L.Q. Ge, H. MÖhwald and J.B. Li, *Chem. Phys. Chem.*, **4**, 1351 (2003).
15. L.Q. Ge, H. MÖhwald and J.B. Li, *Biochem. Biophys. Res. Commun.*, **303**, 653 (2003).
16. L.Q. Ge, J.B. Li and H. MÖhwald, *Colloid. Surf. A*, **221**, 49 (2003).
17. S.F. Ai, G. Lu, Q. He and J.B. Li, *J. Am. Chem. Soc.*, **125**, 11140 (2003).
18. D.H. Reneker, A.L. Yarin, H. Fong and S.J. Koombhongse, *Appl. Phys.*, **87**, 4531 (2000).
19. J.M. Deitzel, J. Kleinmeyer, D. Harris and T.N.C. Beck, *Polymer*, **42**, 261 (2001).
20. K. Mueller, J.F. Quinn, A.P.R. Johnston, M. Becker, A. Greiner and F. Caruso, *Chem. Mater.*, **18**, 2397 (2006).
21. L.Q. Ge, C. Pan, H.H. Chen, X. Wang, C. Wang and Z.Z. Gu, *Colloid. Surf. A*, **293**, 272 (2007).
22. L.Q. Ge, X. Wang, Z.C. Tu, C. Pan, C. Wang and Z.Z. Gu, *J. Appl. Phys. (Japan)*, **46**, 6790 (2007).
23. C. Pan, L.Q. Ge and Z.Z. Gu, *Comp. Sci. Technol.*, **67**, 3271 (2007).
24. T.Z. Zhang, L.Q. Ge, X. Wang and Z.Z. Gu, *Polymer*, **49**, 2898 (2008).
25. L.Q. Ge, K. Nagai, Z.Z. Gu, Y. Shimada, H. Nishimura, N. Miyanaga, Y. Izawa, K. Mima and T. Norimatsu, *Langmuir*, **24**, 10402 (2008).
26. Z.Z. Gu, H. Wei and R. Zhang, *Appl. Phys. Lett.*, **86**, 201915 (2005).
27. X. Wang, Y.G. Kim, C. Drew, B.C. Ku, J. Kumar and L.A. Samuelson, *Nano Lett.*, **4**, 2 (2004).